

Preliminary Sunyaev Zel’dovich Observations of Galaxy Clusters with OCRA-p

Katy Lancaster¹, Mark Birkinshaw¹, Marcin P. Gawroński³, Ian Browne², Roman Feiler³, Andrzej Kus³, Stuart Lowe², Eugeniusz Pazderski³ and Peter Wilkinson²

¹ *University of Bristol, Tyndall Avenue, Bristol BS6 5BX*

² *Jodrell Bank Observatory, University of Manchester, Macclesfield, Cheshire SK11 9DL*

³ *Torun Centre for Astronomy, Nicolaus Copernicus University, ul. Gagarina 11, 87-100 Torun, POLAND*

Received ****insert****; Accepted ****insert****

ABSTRACT

We present 30 GHz Sunyaev Zel’dovich (SZ) observations of a sample of four galaxy clusters with a prototype of the One Centimetre Receiver Array (OCRA-p) which is mounted on the Torun 32-m telescope. The clusters (C10016+16, MS 0451.6-0305, MS 1054.4-0321 and Abell 2218) are popular SZ targets and serve as commissioning observations. All four are detected with clear significance ($4 - 6\sigma$) and values for the central temperature decrement are in good agreement with measurements reported in the literature. We believe that systematic effects are successfully suppressed by our observing strategy. The relatively short integration times required to obtain these results demonstrate the power of OCRA-p and its successors for future SZ studies.

Key words: cosmology:observations – cosmic microwave background – galaxies:clusters:individual (C10016+16, MS 0451.6-0305, MS 1054.4-0321, A2218) – methods:observational

1 INTRODUCTION

The SZ effect is a spectral distortion of the Cosmic Microwave Background (CMB) caused by the inverse Compton scattering of CMB photons off the hot plasma found in clusters of galaxies. At low radio frequencies the SZ effect manifests itself as a fractional decrement in the CMB of order 10^{-4} , whereas at frequencies greater than ~ 220 GHz an increment is observed.

Since the first SZ detections in the 1970s (Birkinshaw et al. 1978) much progress has been made. Extensive interferometric studies have been undertaken, from the first SZ images (Jones et al. 1993), to the use of cluster samples to perform cosmological studies (e.g. Grego et al. 2001, Reese et al. 2002, Saunders et al. 2003, Jones et al. 2005 and Bonamente et al. 2006). Radiometers (e.g. Myers et al. 1997) and bolometers (e.g. Benson et al. 2004) have also been used to good effect. More recently, purpose-built CMB instruments have proved their worth in SZ studies (Lancaster et al. 2005, Udomprasert et al. 2004), although contamination from primordial anisotropies can severely limit the achievable signal-to-noise ratio.

Measurements of the thermal and kinematic SZ effects are studied for the unique information that they can provide on cosmology and the structures of cluster atmospheres (see

reviews of Birkinshaw 1999 and Carlstrom et al. 2002). Although most work in the field of SZ studies to date has been performed using non-ideal instruments, numerous purpose-built SZ observatories are currently under construction (e.g. AMiBA (Lo et al. 2000), AMI (Kneissl et al. 2001), SZA (Loh et al. 2005), ACT (Kosowsky 2003) and SPT (Ruhl 2004)) all with the common aim of performing blind surveys. Such work will exploit the unique redshift-independence of the SZ effect to produce catalogues which are essentially mass-limited, and thus less affected by the biases which plague selection via optical or X-ray methods. Studies of number counts will be used to further constrain the cosmological model and study cluster evolution from formation until the present. Those telescopes which have the capability to produce high-quality imaging will additionally provide the opportunity to better understand cluster physics.

OCRA (Browne et al. 2000) is a planned 100-element continuum receiver which will have excellent surveying and imaging capabilities, and will thus be ideal for performing blind surveys in order to study radio source populations and SZ clusters. The prototype for OCRA, OCRA-p, is a two-element receiver mounted on the 32-m telescope at the Torun Centre for Astrophysics of the Nicolaus Copernicus University, Poland. Even at this preliminary stage, while the

instrument concept is being tested, high-sensitivity SZ measurements are possible, with imaging and surveying planned for the future. We here present our first observations of 4 well-studied massive SZ clusters (Cl0016+16, MS0451.6-0305, MS1054.4-0321 and A2218).

The structure of this paper is as follows. In Section 2 we give a brief description of the Torun 32-m telescope and the OCRA-p receiver. Section 3 contains details of the cluster sample. The observations and data reduction are described in Section 4, and the problem of radio source contamination is detailed in Section 5. Section 6 presents our results and discussion. Throughout the paper we adopt the following cosmological parameter values: $H_0 = 70 \text{ km s}^{-1} \text{ Mpc}^{-1}$, $\Omega_{\text{m}0} = 0.3$, $\Omega_{\Lambda 0} = 0.7$

2 THE TORUN TELESCOPE AND OCRA-P

The Torun observatory is located in Piwnice, 15 km outside Torun in northern Poland. The telescope consists of a 32-m parabolic dish and 3.2-m sub-reflector, with a fully steerable classical Alt-Az mount. It has receivers operating at 1.4-1.7, 5, 6.8, 12 and now, with OCRA-p, 30 GHz. The telescope is used for a variety of studies including interstellar molecules (e.g. Błazkiewicz & Kus 2004), and VLBI (e.g. Bartkiewicz et al. 2005).

The OCRA prototype, OCRA-p, is funded by a grant from the Royal Society Paul Instrument fund. The instrument is described in detail in Lowe (2005) and Lowe et al. (2007); here we present a short summary. The basic radiometer design is based on the prototype for the Planck Low Frequency Instrument (LFI, Mandolesi et al. (2000)), and is similar to the WMAP K-band receivers (Jarosik et al. 2003). OCRA-p consists of two horn-feeds, the beams of which are separated by $3'.1$ and have FWHM $1'.2$. As the beam separation is small, it is possible to reduce the effects of atmospheric and gain fluctuations by switching between the input channels and taking the difference. This can be improved upon by further levels of switching. The full switching strategy for SZ observations is described in Section 4.1.

3 THE CLUSTER SAMPLE

For these preliminary observations, we have chosen four clusters which have well-studied SZ effects, and which cover a wide range of declinations, in order to assess the performance of the telescope/receiver combination. In a future paper we will present results from observations of a large, statistically-complete sample of clusters, observations of which are underway. The cluster sample, and its X-ray properties, is summarised in Table 1.

Our four chosen clusters have been studied at radio wavelengths by a variety of groups employing wide-ranging techniques. In the subsequent sections we summarise previous work in terms of the most recent, any that is close to our observing frequency, and any that employs a similar observing strategy. These clusters have also been studied in detail in X-rays. We note briefly the interesting characteristics reported in the literature, paying particular attention to those which may affect the SZ decrement. We also report

detections of lensing by our target clusters where appropriate.

3.1 Cl0016+16

Cl0016+16 was observed by the pioneers of SZ astronomy, and continues to be a popular target. The SuZIE team performed simultaneous bolometric observations in three frequency bands (145, 221 and 355 GHz) and find a central Comptonisation parameter y_0 of $(3.27^{+1.45}_{-2.86}) \times 10^{-4}$ (Benson et al. 2004), thus $\Delta T_0 = -1785^{+792}_{-1616} \mu\text{K}$. The work of Tsuboi et al. (2004) is interesting, as they employ similar observing techniques to those described in this work. They find a central decrement of $-1431 \pm 133 \mu\text{K}$ using the Nobeyama 45-m telescope, at 43 GHz. Reese et al. (2002) find a similar result of $-1242 \pm 105 \mu\text{K}$, observing with the OVRO and BIMA interferometers at 30 GHz.

Worrall & Birkinshaw (2003) present analysis of an *XMM-Newton* observation of Cl0016+16. They find a best fitting temperature of $9.13^{+0.24}_{-0.22} \text{ keV}$ within 1.5 arcmin of the cluster centre (see Table 1), and note the existence of a central structure which may have a harder spectrum. This, along with the presence of an emission region to the west, may be evidence of merger activity. They comment that their determination of the total gravitating mass is in good agreement with the value derived from lensing data (Smail et al. 1997), thus supporting assumptions of hydrostatic equilibrium. Combination of their X-ray results with a reanalysis of the SZ data presented in Hughes & Birkinshaw (1998) yields a value for the Hubble constant of $68 \pm 8 \text{ km s}^{-1} \text{ Mpc}^{-1}$ (random error only).

3.2 MS 0451.6-0305

Benson et al. (2004) also observed MS0451.6-0305, finding a central Comptonisation parameter from their multi-frequency data of $(2.84 \pm 0.52) \times 10^{-4}$, corresponding to $\Delta T_0 = -1550 \pm 284 \mu\text{K}$. This cluster was also included in the recent work of Tsuboi et al. (2004), who record a central decrement of $-1201 \pm 184 \mu\text{K}$. MS0451.6-0305 also features in the work of the OVRO/BIMA collaboration. Reese et al. (2002) quote a central decrement from their 30 GHz measurements of $-1431^{+98}_{-93} \mu\text{K}$.

The gas temperature and luminosity of MS0451.6-0305 are given in Table 1. Donahue et al. (2003) analyse a Chandra observation in order to obtain a single temperature. They extract spectra from annular regions and do not find a significant gradient between the inner and outer regions of the cluster using these data. However, they also find an acceptable fit to a two-temperature plasma model, although the associated cool component would not contribute significantly to the X-ray emission. Sand et al. (2005) identify 6 candidate lensing arcs in MS0451.6-0305.

3.3 MS 1054.4-0321

MS1054.4-0321 is less well-studied at radio wavelengths. It was observed recently by Benson et al. (2004), who find the central Comptonisation parameter to be $y_0 = (3.87^{+1.19}_{-1.12}) \times 10^{-4}$ from the measurements at 145 GHz. This corresponds to a temperature decrement of $2113^{+650}_{-612} \mu\text{K}$. This cluster

Cluster	RA (J2000)	DEC (J2000)	z	L_x (10^{44} erg s $^{-1}$)	T_x (keV)	References
Cl0016+16	00 18 33.30	+16 26 36.00	0.546	22.7	$9.13^{+0.24}_{-0.22}$	j, h, i
MS0451.6-0305	04 54 10.90	-03 01 07.00	0.550	17.5	$8.05^{+0.5}_{-0.4}$	b, f, g
MS1054.4-0321	10 57 00.20	-03 37 27.00	0.823	12.3	$7.2^{+0.7}_{-0.6}$	b, e, e
A2218	16 35 49.10	+66 12 30.00	0.176	9.6	$6.63^{+0.27}_{-0.27}$	a, c, d

Table 1. Basic cluster data. Coordinates correspond to pointing centres, parameters are as listed in the BAX X-ray cluster database. Luminosities refer to the 0.1-2.4 keV ROSAT energy band. References: (a) Struble & Rood 1999, (b) Gioia & Luppino 1994, (c) Balogh et al. 2002, (d) Pratt et al. 2005, (e) Gioia et al. 2004, (f) Donahue et al. 2003, (g) Tozzi et al. 2003 (h) Ellis & Jones 2002, (i) Worrall & Birkinshaw 2003, (j) Dressler & Gunn 1992.

has also been observed at 30 GHz using the OVRO/BIMA arrays. Joy et al. (2001) use the SZ data to infer a cluster temperature of $10.4^{+5.0}_{-2.0}$ keV, whereas Grego et al. (2001) calculate the gas mass fraction within r_{500} (where r_{500} is the radius inside which the cluster density is greater than 500 times the critical density) to be $f_g = 0.053 \pm 0.028$.

Jee et al. (2005) present a joint analysis of Chandra and HST weak lensing data for this cluster. They find three dominant clumps in the dark matter distribution, and observe that one substructure is not present in the X-ray data. The remaining two features are displaced in the X-rays relative to the HST shear map, probably as a result of a current merger. They find consistent mass estimates ($r < 1$ Mpc), using the datasets independently, of $\sim 1 \times 10^{15} M_\odot$. They also report a significant temperature gradient, but comment that no shock-heated region is observed between the X-ray peaks.

3.4 Abell 2218

A2218 was one of the first clusters to be detected via the SZ effect in the 1970s, and has been studied in much detail since. Most recently, Jones et al. (2005) observed the cluster at 15 GHz with the Ryle telescope, and found a maximum central decrement of $-760 \pm 150 \mu\text{K}$. Reese et al. (2002) record a central decrement of $-731^{+125}_{-150} \mu\text{K}$. Tsuboi et al. (1998) observed this cluster, this time at 36 GHz, and measured the SZ effect to be $-680 \pm 190 \mu\text{K}$.

A2218 has been studied extensively at X-ray wavelengths, and has an X-ray luminosity of 9.55×10^{44} erg s $^{-2}$ and an average gas temperature of 6.63 ± 0.27 keV. A Chandra study of BCS clusters including A2218 is presented in Bauer et al. (2005). They find that the cluster exhibits a cool core. This cluster is also part of a HST lensing study (Smith et al. 2005). The authors combine strong and weak lensing information in order to deduce a total cluster mass of $(5.6 \pm 0.1) \times 10^{14} M_\odot$. Using additional information from archival Chandra observations, they compare the mass and X-ray morphology of the cluster to establish quantitatively that it appears dynamically immature. This is supported by other Chandra studies, such as that reported in Govoni et al. (2004). This work reinforces previous claims that A2218 has an irregular temperature structure, despite its relatively symmetric X-ray morphology.

4 OBSERVATIONS AND DATA REDUCTION

4.1 Observing Strategy

The observations presented in this paper were performed at intervals between June 2005 and April 2006. We aimed to achieve a similar noise level for all clusters, thus observing times were roughly 11 hours for each. The time spent on the cluster itself was less than half of this value due to telescope control issues which have since been resolved. Changes in the atmosphere are problematic for single-dish experiments, and we employ a differencing technique in order to remove the resulting effects. For each cluster we make two observations, firstly the cluster itself (hereafter referred to as the TARGET field) and secondly a trailing field (hereafter referred to as the TRAIL field) at the same declination but offset in right ascension. To this TARGET-TRAIL strategy we apply both beam switching and position switching.

Firstly for the TARGET field, the horn-feeds are positioned such that one beam, beam *A*, is coincident with the cluster centre and the other, beam *B* provides a measure of the blank sky signal. (For extended sources, beam *B* may measure a small signal itself. This must be properly accounted for - see Section 4.4.) We switch between the *A* and *B* beams at a rate of 280 kHz, recording the integrated *A* - *B* difference every second. The beams are repositioned every 53 seconds such that beam *B* measures the cluster and beam *A* measures the sky background, and the differencing is repeated. We then take the double-difference, i.e. $(A_1 - B_1) - (B_2 - A_2)$, such that we recover twice the cluster signal relative to the two background regions. This process is then repeated for a TRAIL field, which is observed over the same range of hour angle as the TARGET field. We are satisfied that our TRAIL fields contain at worst negligible amounts of contaminant signal and thus retain the data purely as a check.

4.2 Calibration

The data are calibrated against an internal noise source, which is itself calibrated via observations of the well-known bright radio sources NGC7027 and 3C286 with assumed flux densities 5.64 Jy^{-1} and 2.51 Jy . Significant changes in the level of the internal noise source occurred over the duration of these observations. Some were due to changes in the

¹ We note that this value, extrapolated to 30 GHz via the scale of Baars et al. (1977), is 3.5% lower than the measurements of Mason et al. (1999). This is well below our systematic error level of 5%.

way that the noise source was used, but others were due to a temperature sensitivity of the noise source, which was controlled by improving the temperature stability in the receiver cabin. Residual uncertainties in the calibration of the system at the level of 5% may be expected.

4.3 Statistical Data Analysis

After combination of the second-by-second average data into double-differenced measurements of the brightness of the sky, and calibration, the data are examined for periods of increased noise (which might arise from receiver instabilities or bad weather conditions) or individual anomalous points. The quality of the data throughout the observing period was good, with a tendency to show a slight increase in noise in Spring 2006 as the weather became warm and wet: weather effects were minimized by the bulk of the observations being taken in visually clear conditions.

The combination of the data into final averages was performed including statistical tests for outlier data. The fractions of the data points rejected by 3σ or 5σ cuts were small in all cases, and no cut-dependent changes in the average results were seen. The distributions of data values in the double-difference data are close to Gaussian, with a slight tendency to show elevated wings in the distributions: the estimates of the error on the mean (Table 4) take account of these deviations from Gaussian distributions.

4.4 Removal of Instrumental Signature

As mentioned in Section 4.1, the small separation of the OCRA-p beams relative to the extent of a cluster’s SZ decrement leads to a significant reduction in the measured signal compared to the intrinsic central signal. In order to remove this effect and recover the ‘true’ SZ signal, we adopt the standard β -model approach. We take values for the core radius r_c and β from the literature (see Table 2) in order to estimate the fraction, F of the SZ signal measured by beams A and B respectively, given where the beams fall on the sky, and thus the fraction of the true signal which we expect to measure with the OCRA-p system. We can then estimate the SZ signal which would be measured by an ‘ideal’ instrument with narrow beams at infinite separation. (We note that the spherical model is non-ideal, but argue that in this context the adverse effects are small given that our observations are restricted to the central regions of the clusters. For more detailed analysis in the future we will adopt more realistic models, but do not feel that it is necessary here). We also account for the parallactic angle range for each set of observations. The results are recorded in Table 2. It is interesting to note that F is very similar (and close to 0.5) for all clusters in the sample despite the large range of redshifts involved. This flatness of response is a generic feature of many practical SZ observing techniques (see, e.g., Birkinshaw & Lancaster 2005).

5 RADIO SOURCE CONTAMINATION

Radio source contamination remains a significant problem for Sunyaev Zel’dovich observations. Here interferometers have a distinct advantage over single-dish experiments as

they offer the possibility of Fourier filtering. Techniques for implementing this method are discussed in Grainger et al. (2002) and Reese et al. (2002). For an instrument such as OCRA-p which operates a position switching strategy, radio sources can affect the data by producing a *positive* signal when they lie close to the cluster centre, or a rogue *negative* signal when they lie in the reference beam of the telescope. If we know the source flux densities at our observing frequency, we can correct the data and establish the true magnitude of the SZ effect for each cluster.

No high-frequency survey of the radio sky exists, but for the four well-known clusters used for our commissioning program we turn to the extensive SZ work reported in the literature. We are fortunate that the OVRO/BIMA group have observed all clusters in our sample at 28.5 GHz or 30 GHz, or both. We make use of the results reported in Cooray et al. (1998), Reese et al. (2002) and Coble et al. (2006). The primary beams of OVRO and BIMA are $4'.2$ and $6'.6$ respectively, and so cover the full fields of relevance for OCRA-p. We also consult the all-sky NVSS (Condon et al. 1998, 1.4 GHz) and GB6 (Gregory et al. 1996, 4.85 GHz) catalogues, plus the 5 GHz observations made by Moffet & Birkinshaw (1989). We consider all sources within $5'$ of the pointing centre for each cluster.

All potentially problematic sources are listed in Table 3. Additionally, the source positions relative to the telescope beams are plotted on RA–dec axes in Figure 1. The greyscale illustrates the arcs generated by the moving blank-sky beams, and the density of points is proportional to the observing time spent at each parallactic angle. The central circle marks the position of the ‘on’ beam at all times.

We apply corrections to our SZ data based on the positions and flux densities of the radio sources in each field. Where we have a measurement of a source at 30 GHz, we use the value directly. For the sources for which information is available at two or more lower frequencies, we fit a simple spectrum and extrapolate to estimate the 30 GHz flux density. Although this method is non-ideal, we note that the error introduced by extrapolating from 28.5 to 30 GHz is likely to be very small. Where only one measurement is available, we adopt a cautious approach and run our correction software twice: once using only the sources detected by OVRO/BIMA, and again using an upper limit on the 30 GHz flux. Contamination through sources at 30 GHz is generally low for bright clusters, producing only small corrections to the SZ data, and thus introducing little bias as a result of the limitations of the methods employed. We do not make any allowance for source variability - this is discussed further in Section 6.

We now examine the radio environment for each cluster in turn, and outline the procedure adopted for each.

5.1 Cl0016+16

We find no sources within $5'$ of Cl0016+16 and thus no correction to the SZ measurement is required.

5.2 MS 0451.6-0305

For MS 0451.6-0305, source 1 lies inside the reference arc, and source 2 approximately one beamwidth outside. We are

Cluster	r_c (arcsec)	β	Offset (arcsec)	F	Refs
Cl0016+16	36.6 ± 1.1	0.697 ± 0.010	30.9	0.52	a
MS 0451.6-0305	45.1 ± 1.2	0.88 ± 0.02	17.6	0.53	b
MS 1054.4-0321	$53.4^{+22.2}_{-12.6}$	$0.96^{+0.48}_{-0.22}$	21.7	0.55	c
A2218	56.0 ± 0.84	0.591 ± 0.004	28.4	0.43	b

Table 2. β -model parameters, estimated offset of pointing centre from apparent X-ray centre, and the estimated fraction of SZ flux measured by the OCRA-p two-beam system. β -model parameters taken from (a) Worrall & Birkinshaw (2003), (b) De Filippis et al. (2005), (c) Neumann & Arnaud (2000)

fortunate to have a 30 GHz flux density measurement for source 1 which we use directly. Source 2 is detected only in the NVSS catalogue. It is conceivable that this source is lost in the noise of the OVRO/BIMA maps, and thus we run our correction software twice: once without the additional source, and again using an upper limit for its flux density. The value for the upper limit is taken as three times the RMS quoted for source 1, 0.78 ± 0.26 mJy. Our measurements are unaffected by the presence (or absence) of this source, since it lies outside the reference arc and has a low flux density.

5.3 MS 1054.4-0321

We find four possible contaminant sources in the MS 1054.4-0321 field. Source 1 lies close to the pointing centre. Source 3 is found inside the reference arc so may also be a problem, although it will enter with low weight. Sources 2 and 4 lie outside and inside the reference arcs respectively. We have 28.5 GHz measurements for sources 1, 3, and 4 which we combine with the NVSS values at 1.4 GHz in order to estimate 30 GHz fluxes as before. For the remaining source, we apply a similar approach to that used for MS 0451.6-0305. We place an upper limit of 0.12 ± 0.04 mJy and re-run the source correction procedure. Again we find that the presence/absence of this source does not affect our measurement, despite its position in the reference arc, presumably to the low value of the upper limit placed on its flux density.

5.4 A2218

A2218 has been observed at 30 GHz, and three sources are detected. We use these flux densities directly.

6 RESULTS AND DISCUSSION

Our SZ measurements are presented in Table 4. Column two contains the double-differenced values measured for the TARGET field for each cluster. Column three lists the same values for the TRAIL fields, which we note are generally consistent with zero. As mentioned in Section 4.1, we feel that this eliminates the need for our third level of differencing and subsequently will use the TRAIL measurements as a check only. We illustrate our data via the cumulative histograms presented in Figure 2. For each cluster, the TARGET data are clearly shifted towards negative values relative to the TRAIL data, indicating clear detections. We apply a standard two-sided Kolmogorov-Smirnov test and verify that at the 1% level, the measurements from the TARGET fields have different distributions from the TRAIL fields.

The double-differenced values in column two of Table 4

represent only a fraction of the actual SZ signal (as discussed in Section 4.1). We list flux density values after correction (see Section 4.4 for the instrumental signature and radio source contamination (see Section 5) in column four. Central temperature decrements are summarised in column five, with the amount of telescope time listed in column six (note that this is roughly twice the actual integration time). We achieve clear detections of our four well-known clusters.

To facilitate comparison, we also list our results alongside those quoted in Section 3 in Table 5. Our results for Cl0016+16, MS 0451.6-0305, and MS 1054.4-0321 are in good agreement with previous work, affirming that our observing strategy, radio source treatment, and modeling are all effective. The one exception is A2218 which is rather high, although only $\sim 1.5\sigma$ away from the other measurements. However, as discussed in Section 3.4, this cluster displays irregular morphology. With the OCRA beam we may be measuring the SZ signal from a particularly high pressure region. Due to the extended nature of the SZ effect and ambiguities in defining cluster centres, it is likely that our pointing centre differs from those used by the comparison experiments. Additionally, we note that we have not incorporated the possibility of source variability in our analysis. We deduce that this is not a major factor here, given the good agreement between our measurements and those reported in the literature, although this could perhaps provide an alternative explanation for the discrepancy noted above.

The short integration time required to obtain these clear detections demonstrates the power of OCRA-p in SZ studies. We stress that the values quoted in table 4 correspond to the total time required to take the data. The OCRA control system is rather inefficient (although recently improved) and thus the telescope spent more than half of this time off source. The predicted noise on a one second integration of ~ 3.6 mJy degrades by a factor of ~ 2 to the measured value of 7.0 mJy. Integrating over the full ‘on-source’ time of around 3 hours (8478 samples), we would expect this value to reduce to ~ 0.08 mJy, which is better than the measured ~ 0.4 mJy by a factor of 5. This degradation is likely due to non-optimal removal of atmospheric effects, which may partly be attributed to the poor telescope control. With improvements to both the OCRA receiver and the telescope control system, we expect OCRA’s sensitivity to increase substantially in forthcoming observing runs. Over the current season, we have scheduled observations of a large, statistically complete, X-ray selected sample of clusters at $z > 0.2$. These observations will form an SZ catalogue with uniquely well-understood selection effects. This will enable us to test SZ/X-ray scaling relations (e.g. Cooray 1999). The SZ measurements will be combined with high-quality X-ray data in order to further test cluster models. We also

Cluster	Source No.	RA (J2000)	DEC (J2000)	$S_{30.0}$ (mJy)	$S_{28.5}$ (mJy)	S_5 (mJy)	$S_{1.4}$ (mJy)	References
Cl0016+16	-	-	-	-	-	-	--	-
MS 0451.6-0305	1	04 54 22.1	-03 01 25	1.41 ± 0.26	1.86 ± 0.26	...	14.9 ± 0.7	a, a, -, c
	2	04 54 30.53	-03 00 44.5	14.6 ± 0.6	-, -, -, c
MS 1054.4-0321	1	10 56 59.6	-03 37 30	...	0.90 ± 0.04	...	14.1 ± 0.9	-, d, -, c
	2	10 56 48.24	-03 40 04.6	4.6 ± 0.4	-, -, -, c
	3	10 56 48.74	-03 37 25.4	...	1.4 ± 0.04	...	18.2 ± 1.0	-, d, -, c
	4	10 56 57.58	-03 38 54.7	...	0.4 ± 0.04	...	3.1 ± 0.4	-, d, -, c
A2218	1	16 35 22.1	66 13 23	4.29 ± 0.21	4.43 ± 0.20	2.8 ± 0.2	1.25 ± 0.21	a, a, b, b
	2	16 35 47.7	66 14 46	1.36 ± 0.10	1.59 ± 0.11	3.7 ± 0.3	18.0 ± 1.8	a, a, b, c
	3	16 36 16.0	66 14 23	2.41 ± 0.29	3.13 ± 0.30	4.2 ± 0.1	13.3 ± 0.6	a, a, b, c

Table 3. Radio sources associated with each of the six clusters. Fluxes taken from (a) Reese et al. (2002), (b) Moffet & Birkinshaw (1989), (c) Condon et al. (1998), (d) Coble et al. (2006), (e) 4.85 GHz, Gregory et al. (1996). The source index refers to Figure 1.

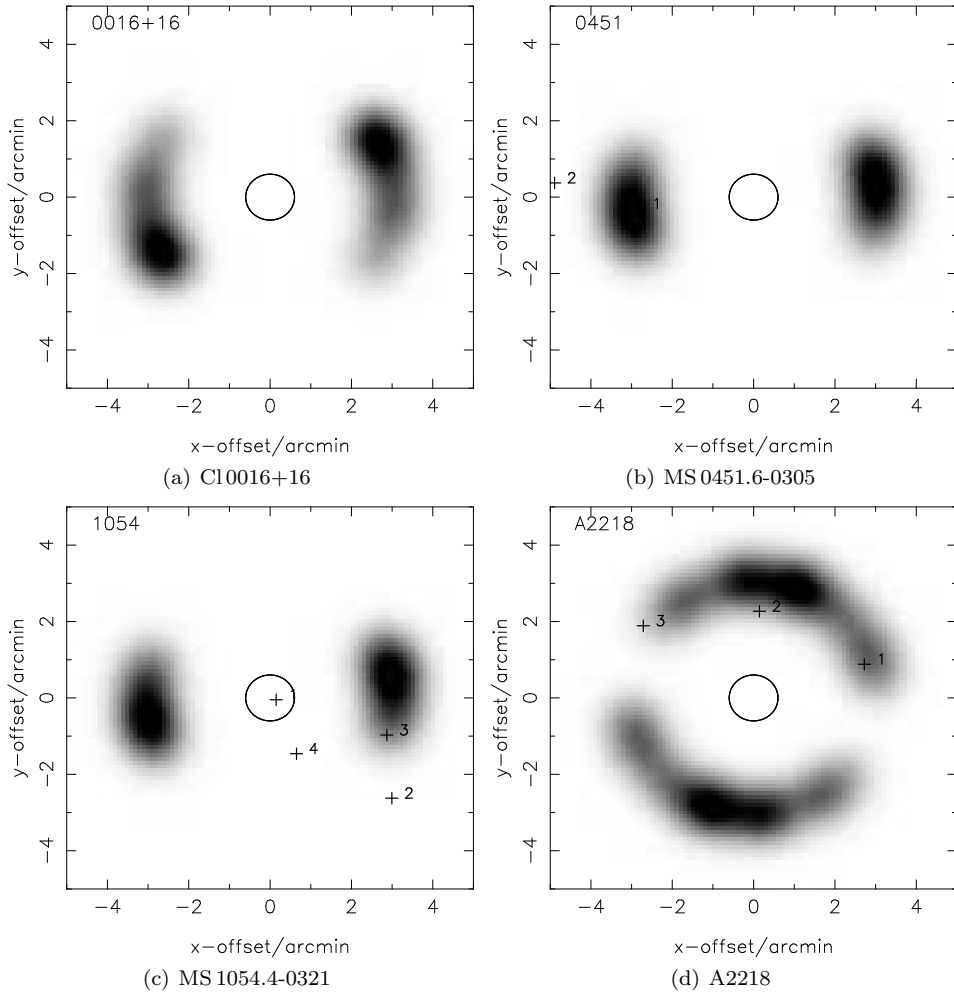


Figure 1. Radio sources in each cluster, shown relative to beams A and B, where the ‘off’ beam B traces arcs as the telescope tracks the cluster. The source numbers correspond to the details presented in Table 3.

Cluster	TARGET flux (mJy)	TRAIL flux (mJy)	S_{SZ} (mJy)	ΔT (μK)	Telescope Time (Hours)
Cl0016+16	-1.884 ± 0.345	0.540 ± 0.411	-4.28 ± 0.78	-1647 ± 302	11.5
MS 0451.6-0305	-2.500 ± 0.425	0.446 ± 0.347	-4.05 ± 0.80	-1558 ± 309	10.5
MS 1054.4-0321	-1.953 ± 0.406	0.331 ± 0.384	-4.48 ± 0.74	-1722 ± 283	13.5
A2218	-1.696 ± 0.317	0.036 ± 0.286	-3.01 ± 0.75	-1159 ± 288	11.0

Table 4. Measured fluxes in the TARGET and TRAIL fields, difference and corrected measurements, and central temperature decrements.

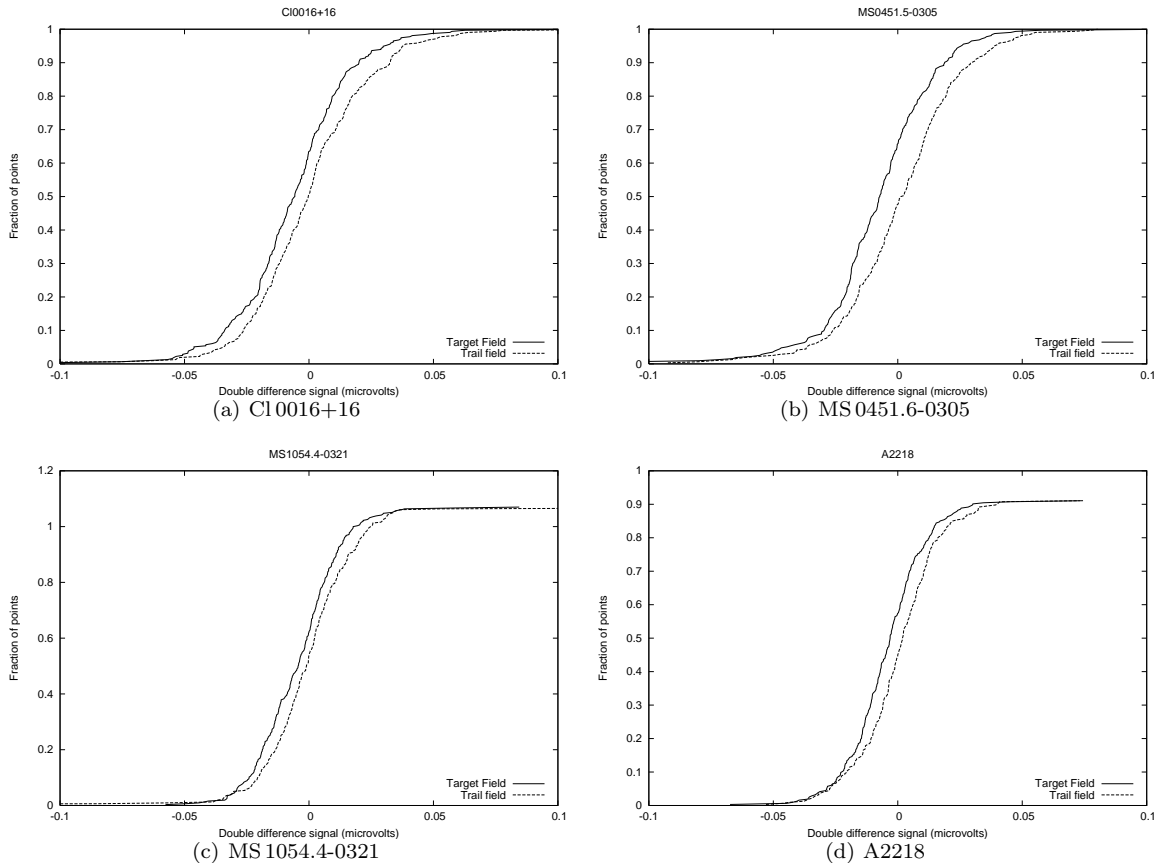


Figure 2. Cumulative histograms illustrating the raw data obtained through observing the Target and Trail fields for each cluster. Note the negative shift of the Target curve relative to the Trail curve, indicating clear SZ detections. In each case, the distributions are clearly separated by a standard Kolmogorov–Smirnov test.

anticipate performing observations of high-redshift cluster candidates found by the *XMM-Newton* Large Scale Structure survey such as that reported by Bremer et al. (2006). The two samples will be at significantly different mean redshifts, thus facilitating studies of the evolution of cluster properties. The OCRA-p commissioning observations also pave the way for SZ imaging. It is possible, by means of numerous pointings, to map clusters using OCRA-p. However, a multiple-beam instrument such as OCRA-F would be far more efficient. The installation of OCRA-F on the telescope will allow us to make the first well-resolved maps of SZ clusters with OCRA-F after summer 2007.

OCRA-F, and indeed the full, 100-beam instrument, will also be used to perform blind surveys for galaxy clusters. Some source correction will be possible via follow-up observations of suspected sources present in the reference beam traces. Deeper observations, coupled with reference arc analysis, would allow contaminant sources to be detected and

removed provided that the data are taken over a sufficiently large range of parallactic angles. Naturally, there may be some cases where sufficient additional information about possible contaminant sources is not available. For clusters as massive as the four discussed here, we do not expect radio sources to preclude detection. If we were to ignore the source corrections, all four clusters would still be unambiguously detected, and the temperature decrements would remain close to the values reported in the literature. Cl0016+16 has no source contamination so is unchanged. The ΔT values for MS 0451.6-0305 and A2218 become rather high as a result of switching onto sources in the reference arcs ($-1814 \pm 308 \mu K$ and $-1517 \pm 284 \mu K$ respectively) while MS 1054.4-0321 is low due to the central radio source ($-1366 \pm 284 \mu K$).

As we move towards observing fainter clusters, we recognise that contamination by primordial CMB features could potentially be a problem, as noted in other work (e.g. Lancaster et al. 2005). However, OCRA is a relatively high-

resolution instrument, probing arcminute scales which correspond to $3500 \lesssim \ell \lesssim 10000$. At such high multipoles, for a concordance cosmology and including the effects of lensing, we expect the amplitude of the temperature power spectrum to be of the order of a few μK . This would be well below the OCRA noise in surveys of scale ~ 100 square degrees with planned sensitivity of $\sim 100 \mu\text{K}$.

7 ACKNOWLEDGMENTS

We acknowledge support for the design and construction of OCRA-p from the Royal Society Paul Instrument Fund, and funds for the data acquisition system and operation on the telescope from the Ministry of Science in Poland via grant number KBN 5 P03D 024 21 who, along with PPARC, also supported the scientific exploitation of the completed system. We thank Anze Slosar for useful discussions. Finally, we thank the anonymous referee for their valuable input.

REFERENCES

- Baars J. W. M., Genzel R., Pauliny-Toth I. I. K., Witzel A., 1977, *A&A*, 61, 99
- Balogh M. L., Smail I., Bower R. G., Ziegler B. L., Smith G. P., Davies R. L., Gaztelu A., Kneib J.-P., Ebeling H., 2002, *ApJ*, 566, 123
- Bartkiewicz A., Szymczak M., van Langevelde H. J., 2005, *A&A*, 442, L61
- Bauer F. E., Fabian A. C., Sanders J. S., Allen S. W., Johnstone R. M., 2005, *MNRAS*, 359, 1481
- Benson B. A., Church S. E., Ade P. A. R., Bock J. J., Ganga K. M., Henson C. N., Thompson K. L., 2004, *ApJ*, 617, 829
- Birkinshaw M., 1999, *Phys.Rep.*, 310, 97
- Birkinshaw M., Gull S. F., Northover K. J. E., 1978, *Nature*, 275, 40
- Birkinshaw M., Lancaster K., 2005, in Melchiorri F., Rephaeli Y., eds, *Background Microwave Radiation and Intracluster Cosmology Observational issues in radiometric and interferometric detection and analysis of the Sunyaev-Zel'dovich effects*. pp 127–+
- Blażkiewicz L., Kus A. J., 2004, *A&A*, 413, 233
- Bonamente M., Joy M. K., LaRoque S. J., Carlstrom J. E., Reese E. D., Dawson K. S., 2006, *ApJ*, 647, 25
- Bremer M. N., Valtchanov I., Willis J., Altieri B., Andreon S., Duc P. A., Fang F., Jean C., Lonsdale C., Pacaud F., Pierre M., Shupe D. L., Surace J. A., Waddington I., 2006, *MNRAS*, 371, 1427
- Browne I. W., Mao S., Wilkinson P. N., Kus A. J., Marecki A., Birkinshaw M., 2000, in Butcher H. R., ed., *Proc. SPIE Vol. 4015*, p. 299-307, *Radio Telescopes*, Harvey R. Butcher; Ed. OCRA: a one-centimeter receiver array. pp 299–307
- Carlstrom J. E., Holder G. P., Reese E. D., 2002, *ARA&A*, 40, 643
- Coble K., Carlstrom J. E., Bonamente M., Dawson W., Holzapfel M., Joy M., LaRoque S., Reese E. D., 2006, *Radio Point Sources Toward Galaxy Clusters at 30 GHz*, preprint, [astro-ph/0608274](http://arxiv.org/abs/astro-ph/0608274)
- Condon J. J., Cotton W. D., Greisen E. W., Yin Q. F., Perley R. A., Taylor G. B., Broderick J. J., 1998, *AJ*, 115, 1693
- Cooray A. R., 1999, *MNRAS*, 307, 841
- Cooray A. R., Grego L., Holzapfel W. L., Joy M., Carlstrom J. E., 1998, *AJ*, 115, 1388
- De Filippis E., Sereno M., Bautz M. W., Longo G., 2005, *ApJ*, 625, 108
- Donahue M., Gaskin J. A., Patel S. K., Joy M., Clowe D., Hughes J. P., 2003, *ApJ*, 598, 190
- Dressler A., Gunn J. E., 1992, *ApJS*, 78, 1
- Ellis S. C., Jones L. R., 2002, *MNRAS*, 330, 631
- Gioia I. M., Braito V., Branchesi M., Della Ceca R., Maccauro T., Tran K.-V., 2004, *A&A*, 419, 517
- Gioia I. M., Luppino G. A., 1994, *ApJS*, 94, 583
- Govoni F., Markevitch M., Vikhlinin A., VanSpeybroeck L., Feretti L., Giovannini G., 2004, *ApJ*, 605, 695
- Grainger W. F., Das R., Grainge K., Jones M. E., Kneissl R., Pooley G. G., Saunders R. D. E., 2002, *MNRAS*, 337, 1207
- Grego L., Carlstrom J. E., Reese E. D., Holder G. P., Holzapfel W. L., Joy M. K., Mohr J. J., Patel S., 2001, *ApJ*, 552, 2
- Gregory P. C., Scott W. K., Douglas K., Condon J. J., 1996, *ApJS*, 103, 427
- Hughes J. P., Birkinshaw M., 1998, *ApJ*, 501, 1
- Jarosik N., Bennett C. L., Halpern M., Hinshaw G., Kogut A., Limon M., Meyer S. S., Page L., Pospieszalski M., Spergel D. N., Tucker G. S., Wilkinson D. T., Wollack E., Wright E. L., Zhang Z., 2003, *ApJS*, 145, 413
- Jee M. J., White R. L., Ford H. C., Blakeslee J. P., Illingworth G. D., Coe D. A., Tran K.-V. H., 2005, *ApJ*, 634, 813
- Jones M. E., Edge A. C., Grainge K., Grainger W. F., Kneissl R., Pooley G. G., Saunders R., Miyoshi S. J., Tsurutu T., Yamashita K., Tawara Y., Furuzawa A., Harada A., Hatsukade I., 2005, *MNRAS*, 357, 518
- Jones M. E., Saunders R., Alexander P., Birkinshaw M., Dillon N., Grainge K., Hancock S., Lasenby A., Lefebvre D., Pooley G., 1993, *Nature*, 365, 320
- Joy M., LaRoque S., Grego L., Carlstrom J. E., Dawson K., Ebeling H., Holzapfel W. L., Nagai D., Reese E. D., 2001, *ApJ*, 551, L1
- Kneissl R., Jones M. E., Saunders R., Eke V. R., Lasenby A. N., Grainge K., Cotter G., 2001, *MNRAS*, 328, 783
- Kosowsky A., 2003, *New Astronomy Reviews*, 47, 939
- Lancaster K., Genova-Santos R., Falcón N., Grainge K., Gutiérrez C., Kneissl R., Marshall P., Pooley G., Rebolo R., Rubiño-Martin J.-A., Saunders R. D. E., Waldram E., Watson R. A., 2005, *MNRAS*, 359, 16
- Lo K. Y., Chiueh T., Martin R. N., 2000, *Bulletin of the American Astronomical Society*, 32, 1497
- Loh M., Carlstrom J. E., Cartwright J. K., Greer C., Hawkins D., Hennessy R., Joy M., Lamb J., Leitch E., Miller A., Mroczkowski T., Muchovej S., Pryke C., Reddall B., Richardson G., Runyan M., Sharp M., Woody D., 2005, *Bulletin of the American Astronomical Society*, 37, 1225
- Lowe S., 2005, PhD thesis, University of Manchester
- Lowe S. R., Gawroński M., Wilkinson P. N., Kus A. J., Browne I. W. A., Pazderski E., Feiler R., 2007, *30 GHz flux density measurements of the CJF sources with*

		ΔT (μK)		
Cl0016+16	MS 0451.6-0305	MS 1054.4-0321	A2218	References
-1647^{+302}_{-302}	-1558^{+309}_{-309}	-1722^{+283}_{-283}	-1159^{+288}_{-288}	OCRA
-1785^{+792}_{-1616}	-1550^{+284}_{-284}	-2113^{+650}_{-612}	-	Benson et al. (2004)
-1431^{+133}_{-133}	-1201^{+184}_{-184}	-	-680^{+190}_{-190}	Tsuboi et al. (2004)
-1242^{+105}_{-105}	-1431^{+98}_{-93}	-	-731^{+125}_{-150}	Reese et al. (2002)
-	-	-	-760^{+150}_{-150}	Jones et al. (2005)

Table 5. Comparison of OCRA results for the four clusters with temperature decrements quoted in the literature.

OCRA-p, In preparation

- Mandolesi N., Bersanelli M., Burigana C., Villa F., 2000, *Astrophysical Letters Communications*, 37, 151
- Mason B. S., Leitch E. M., Myers S. T., Cartwright J. K., Readhead A. C. S., 1999, *AJ*, 118, 2908
- Moffet A. T., Birkinshaw M., 1989, *AJ*, 98, 1148
- Myers S. T., Baker J. E., Readhead A. C. S., Leitch E. M., Herbig T., 1997, *ApJ*, 485, 1
- Neumann D. M., Arnaud M., 2000, *ApJ*, 542, 35
- Pratt G. W., Böhringer H., Finoguenov A., 2005, *A&A*, 433, 777
- Reese E. D., Carlstrom J. E., Joy M., Mohr J. J., Grego L., Holzzapfel W. L., 2002, *ApJ*, 581, 53
- Ruhl J., 2004 *The South Pole Telescope*. pp 11–29
- Sand D. J., Treu T., Ellis R. S., Smith G. P., 2005, *ApJ*, 627, 32
- Saunders R., Kneissl R., Grainge K., Grainger W. F., Jones M. E., Maggi A., Das R., Edge A. C., Lasenby A. N., Pooley G. G., Miyoshi S. J., Tsuruta T., Yamashita K., Tawara Y., Furuzawa A., Harada A., Hatsukade I., 2003, *MNRAS*, 341, 937
- Smail I., Ellis R. S., Dressler A., Couch W. J., Oemler A. J., Sharples R. M., Butcher H., 1997, *ApJ*, 479, 70
- Smith G. P., Kneib J.-P., Smail I., Mazzotta P., Ebeling H., Czoske O., 2005, *MNRAS*, 359, 417
- Struble M. F., Rood H. J., 1999, *ApJS*, 125, 35
- Tozzi P., Rosati P., Ettori S., Borgani S., Mainieri V., Norman C., 2003, *ApJ*, 593, 705
- Tsuboi M., Miyazaki A., Kasuga T., Kuno N., Sakamoto A., Matsuo H., 2004, *PASJ*, 56, 711
- Tsuboi M., Miyazaki A., Kasuga T., Matsuo H., Kuno N., 1998, *PASJ*, 50, 169
- Udomprasert P. S., Mason B. S., Readhead A. C. S., Pearson T. J., 2004, *ApJ*, 615, 63
- Worrall D. M., Birkinshaw M., 2003, *MNRAS*, 340, 1261

This paper has been typeset from a \LaTeX file prepared by the author.